

Comparison of dynamics of the 6-wave 1D kinetic equation and corresponding NLSE for finite regions.

A. O. Korotkevich,

in collaboration with: Banks J., Buckmaster T., Kovačič G., Shatah J.,

Department of Mathematics and Statistics, University of New Mexico, USA.
alexkor@math.unm.edu

L. D. Landau Institute for Theoretical Physics RAS, Chernogolovka, Russia.

Supported by **Simons' Collaboration on Wave Turbulence.**

20th of December, 2021,

XXXth Session of the Council on Nonlinear Dynamics RAS.

1D quintic NLSE.

Let's consider quintic defocusing Nonlinear Schrödinger Equation (qNLSE):

$$iu_t + u_{xx} - \mu|u|^4 u = 0,$$

which is relevant in some cases:

- NLSE can be considered as intensity correction to the dispersion relation: $\omega_k = k^2 + \mu|u|^2$ (cubic equation, four waves interaction).
- In 1D case of NLSE (e.g. fiber optics) four waves interactions are non-resonant (no description of wave turbulence in the fiber).
- One needs to look for further term in intensity (nonresonant term can be eliminated by canonical transformation): $\omega_k = k^2 + \mu|u|^4$.
- qNLSE results in 6-waves WKE, which is almost the same for Kelvin waves on superfluid vortices at least on some scales (different dispersion relation $\omega_k \sim k^2 \log(\kappa/k)$).

Interaction of 3-into-3 waves, energy and number of particles are conserved. $x \in [0, L]$, periodic boundary conditions, initial condition $u_0(x)$, $\mu > 0$ (defocusing case).

Fourier transformation.

The dynamics of the spectrum is studied by considering the evolution of the Fourier coefficients $a_k(t)$:

$$u(x, t) = \frac{1}{L} \sum_k a_k(t) e^{i(kx - \omega_k t)}. \quad (1)$$

Here k is a wavenumber, which is an integer multiple of $\Delta k = 2\pi/L$, $\omega_k = k^2$ is the dispersion relation for (2). The equation and the initial condition for (2) can be written as

$$\begin{cases} \dot{a}_k(t) = i \frac{\mu}{L^4} \sum_{S_k=0} \bar{a}_1(t) \bar{a}_2(t) a_3(t) a_4(t) a_5(t) e^{-it\Omega} \\ a_{0k} = c_k e^{i\gamma_k}, \end{cases} \quad (2)$$

where dot over function means time derivative, $\Omega = \omega_k + \omega_{k_1} + \omega_{k_2} - \omega_{k_3} - \omega_{k_4} - \omega_{k_5}$, $S_k = k + k_1 + k_2 - k_3 - k_4 - k_5$, and $a_i = a_{k_i}$.

Weak nonlinearity.

Initial data: $c_k = \text{const} \simeq 1$ in some range of scales $[-k_{max}, k_{max}]$, and γ_k – uniformly distributed I.I.D. random on $[0, 2\pi)$. Let's fix $k_{max} = \frac{1}{2}$ and require the L_2 -norm of the initial condition to be equal to one $\|u_0\|_2 = 1$. By the random phase assumption the L_∞ -norm of the initial condition scales as $\|u_0\|_\infty \sim 1/L^{1/2}$.

The two parameters present in the equation are the size of the domain L and the strength of the nonlinearity μ . It is convenient to express μ in terms of L by writing $\mu = L^p$ and considering (L, p) as the two parameters present in our system. The weakly nonlinear regime, under which wave turbulence theory has physical relevance, can be formulated as:

$$\mu \|u_0\|_\infty^4 = \mu/L^2 = L^{p-2} \ll k_{max}^2, \text{ or } p < 2. \quad (3)$$

Here we used $k_{max} = O(1)$.

Wave Kinetic Equation. Finite period.

One can derive the wave kinetic equation (WKE) for equation (2), which describes dynamics of the spectrum $\langle |a_k|^2 \rangle = n_k$. Taking into account the random phase assumption, and letting $a_\ell^0 = a_\ell(0)$ denote the initial value of a_ℓ , for a short time one gets

$$\begin{aligned} \dot{n}_k \sim & 12 \left(\frac{\mu}{L^4} \right)^2 \sum_{S_k=0} \left(\frac{1}{|a_k^0|^2} + \frac{1}{|a_1^0|^2} + \frac{1}{|a_2^0|^2} \right. \\ & \left. - \frac{1}{|a_3^0|^2} - \frac{1}{|a_4^0|^2} - \frac{1}{|a_5^0|^2} \right) |a_k^0|^2 |a_1^0|^2 \dots |a_5^0|^2 \frac{\sin^2(\frac{\Omega}{2}t)}{(\frac{\Omega}{2})^2}, \end{aligned} \quad (4)$$

where we have ignored higher order terms that decay to zero in the infinite domain limit.

Wave Kinetic Equation. Infinite period.

Taking L to infinity, and taking a continuum limit, we obtain

$$\begin{aligned}
 n_k \sim \frac{t}{\tau_{kin}} \int & n_k^0 n_{k_1}^0 n_{k_2}^0 n_{k_3}^0 n_{k_4}^0 n_{k_5}^0 \left(\frac{1}{n_k^0} + \frac{1}{n_{k_1}^0} + \right. \\
 & \left. + \frac{1}{n_{k_2}^0} - \frac{1}{n_{k_3}^0} - \frac{1}{n_{k_4}^0} - \frac{1}{n_{k_5}^0} \right) \delta(k + k_1 + k_2 - \\
 & - k_3 - k_4 - k_5) \delta(\omega_k + \omega_{k_1} + \omega_{k_2} - \omega_{k_3} - \\
 & - \omega_{k_4} - \omega_{k_5}) dk_1 dk_2 dk_3 dk_4 dk_5
 \end{aligned} \tag{5}$$

where $n_k^0 = n_k(0)$ and $\tau_{kin} = \pi L^4 / (6\mu^2) = \pi L^{4-2p} / 6$ is the kinetic time scale, the time at which the WKE experiences an $O(1)$ change.

Wave Kinetic Equation.

The WKE above is valid for short periods of time Δt , if one takes the limit $\Delta t \rightarrow 0$ the following can be obtained:

$$\begin{aligned} \frac{\partial n_k}{\partial s} = & \int n_k n_{k_1} n_{k_2} n_{k_3} n_{k_4} n_{k_5} \left(\frac{1}{n_k} + \frac{1}{n_{k_1}} + \frac{1}{n_{k_2}} - \frac{1}{n_{k_3}} - \frac{1}{n_{k_4}} - \frac{1}{n_{k_5}} \right) \times \\ & \times \delta(k + k_1 + k_2 - k_3 - k_4 - k_5) \delta(\omega_k + \omega_{k_1} + \omega_{k_2} - \omega_{k_3} - \omega_{k_4} - \omega_{k_5}) \times \\ & \times dk_1 dk_2 dk_3 dk_4 dk_5 \end{aligned} \quad (6)$$

where for convenience, we have renormalized time by setting $s = t/\tau_{kin}$.

Because both energy and number of particles are conserved, we have two fluxes: of energy and number of particles. KZ-solutions are not realized (wrong signs of fluxes, Fjørtoft argument).

Waves Kinetic Equation applicability. Problem formulation.

Because we performed rigorous derivation of WKE, the following questions naturally arise:

- What choice of system parameters is relevant?
- When we break WKE assumptions?
- How boundary conditions influence the problem?

We shall perform simulations in both dynamical and WKE frameworks for the same initial conditions.

A key requirement for validity of the WKE is the weak nonlinearity condition (3), which imposes the inequality $p < 2$ upon taking L large.

Waves Kinetic Equation applicability.

The condition $p < 2$ also arises in a key step in deriving (6) from (4):

$$\frac{\sin^2(\frac{\Omega}{2}t)}{(\frac{\Omega}{2})^2} \xrightarrow{t \rightarrow \infty} 2\pi t \delta(\Omega).$$

Since we will be considering times $t = O(\tau_{kin})$, we will require $\tau_{kin} \gg 1$, which given the definition of τ_{kin} , in the infinite domain limit, again requires that we take $p < 2$. We note that with $p < 2$ fixed, $\tau_{kin} \gg 1$ also provides a practical lower bound on L for our simulations, which degenerates at $p = 2$.

One have to prevent coherent structures from playing the dominant role in the dynamics of the equation. This can be formulated as $\tau_{kin} \ll L^2 \log L$, which gives $p > 1$. Here the RHS appears from estimation of number of exact solutions of Diophantine equation $\Omega = 0$ on a set of integers.

Therefore, in order to ensure that the qNLSE is well approximated by the WKE at the infinite domain limit, we require

$$1 < p < 2.$$

(7)

Initial conditions for WKE.

Equation (6) was solved numerically using an algorithm inspired by Webb-Resio-Tracy (Webb 1978, Tracy and Resio 1982) approach to simulation of WKE for gravity waves. In short, we scan the 6D wavenumbers space and consider only those modes sextets which satisfy resonant conditions (both δ -functions under the integral sign). As initial condition we considered $n_k = 1$ in the interval $k \in [-1/2, 1/2]$ and $n_k = 0$ everywhere else.

Number of harmonics in WKE simulations was 81. For every wavenumber we need to integrate over 5-dimensional space with two bonds (resonant conditions), which results in 3-dimensional space. So time of simulation growth cubically with number of harmonics.

Dynamical equation (qNLSE) was simulated for 1000 realizations of random phases and then $\langle |a_k|^2 \rangle$ compared with n_k from WKE.

Dynamical equations and WKE. $\rho = 1.1$, $L = 20$.

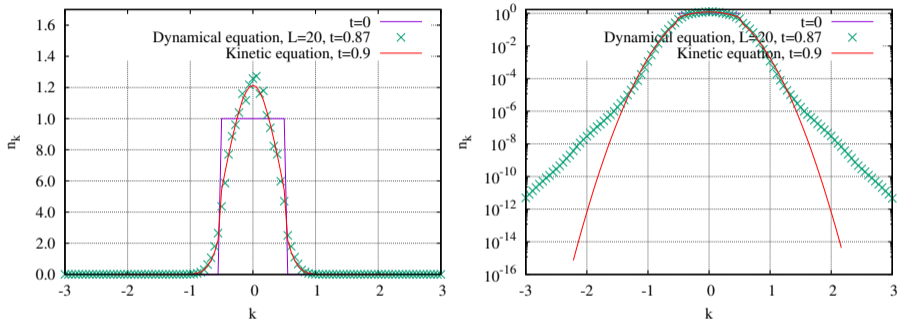


Figure: Comparison of averaged squared amplitudes of harmonics from dynamical simulations with results of simulations in the framework of kinetic equation. Linear and logarithmic scales. Moment of time $s = 0.9$, $\rho = 1.1$, $L = 20$.

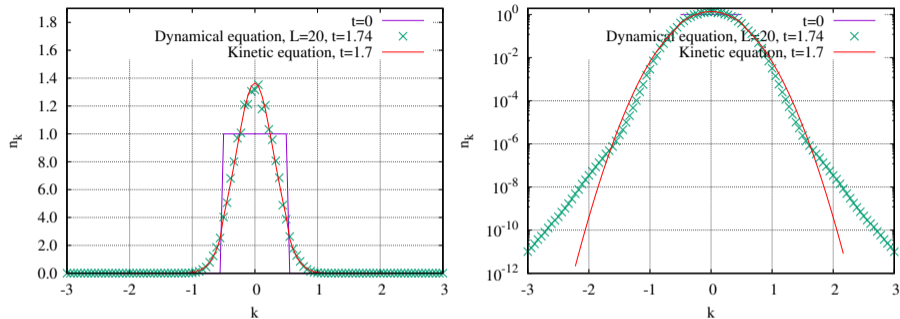


Figure: Comparison of averaged squared amplitudes of harmonics from dynamical simulations with results of simulations in the framework of kinetic equation. Linear and logarithmic scales. Moment of time $t = s.7$, $p = 1.1$, $L = 20$.

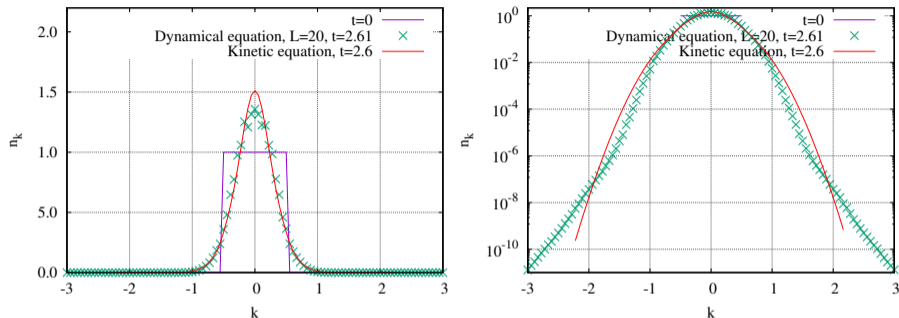


Figure: Comparison of averaged squared amplitudes of harmonics from dynamical simulations with results of simulations in the framework of kinetic equation. Linear and logarithmic scales. Moment of time $s = 2.6$, $p = 1.1$, $L = 20$.

Comparison with dynamical equations. $p = 1.1$, $L = 40$.

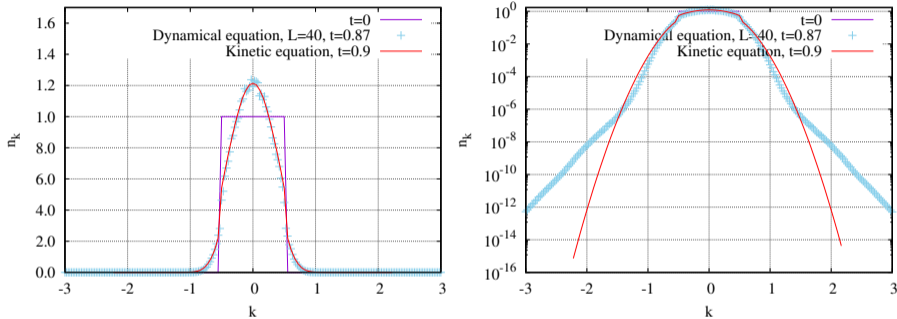


Figure: Comparison of averaged squared amplitudes of harmonics from dynamical simulations with results of simulations in the framework of kinetic equation. Linear and logarithmic scales. Moment of time $s = 0.9$, $p = 1.1$, $L = 40$.

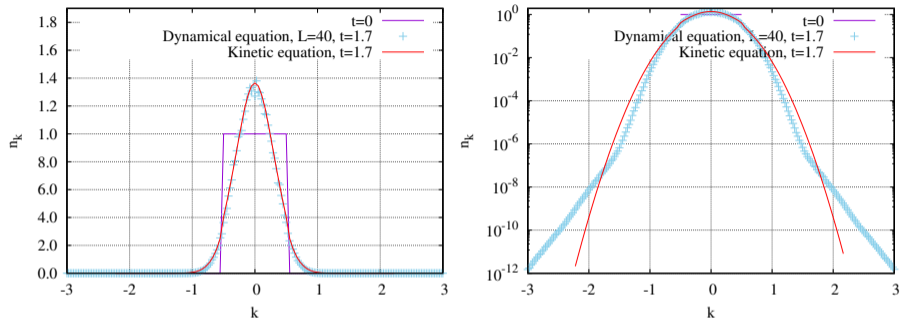


Figure: Comparison of averaged squared amplitudes of harmonics from dynamical simulations with results of simulations in the framework of kinetic equation. Linear and logarithmic scales. Moment of time $s = 1.7$, $p = 1.1$, $L = 40$.

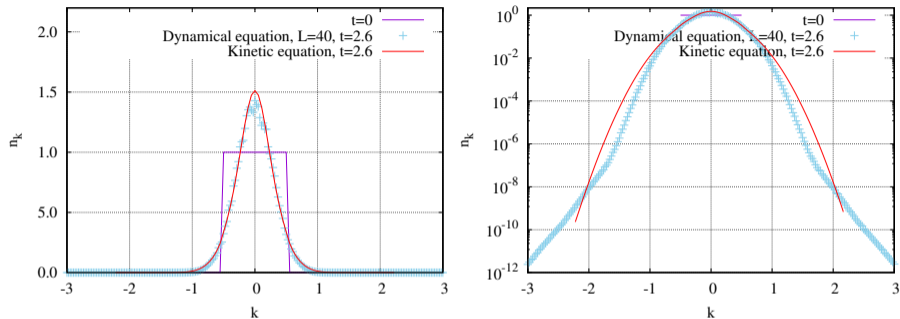


Figure: Comparison of averaged squared amplitudes of harmonics from dynamical simulations with results of simulations in the framework of kinetic equation. Linear and logarithmic scales. Moment of time $s = 2.6$, $p = 1.1$, $L = 40$.

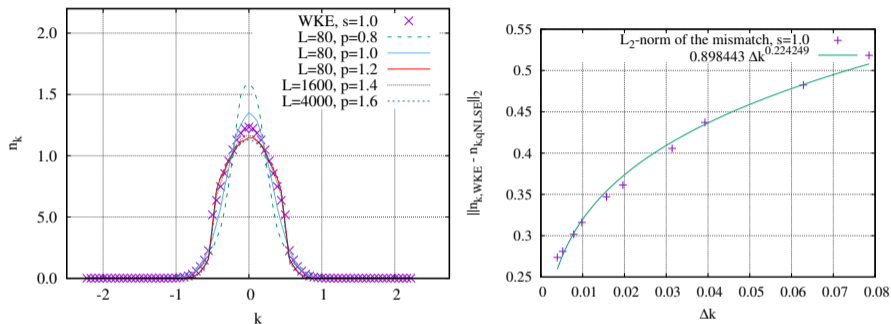
Different values of p .

Figure: (Left panel) Comparison of averaged squared amplitudes of harmonics from simulations of qNLSE and WKE at $t = \tau_{kin}$ or $s = 1$ for different values of parameter p . (Right Panel) L_2 -norm of a mismatch between qNLSE and WKE as a function of $\Delta k \sim 2\pi/L$ for the case $p = 1.4$ at $s = 1$.

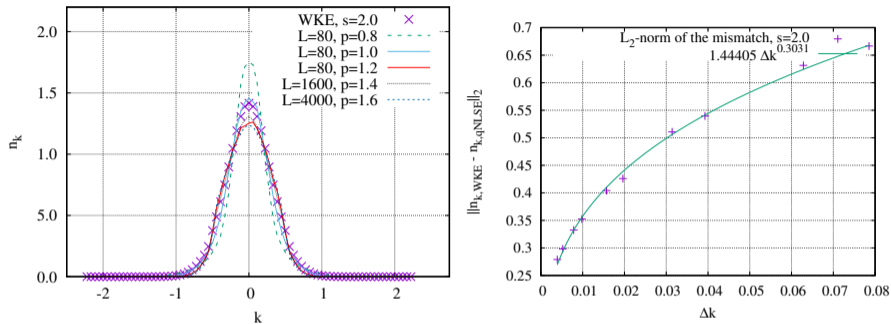


Figure: (Left panel) Comparison of averaged squared amplitudes of harmonics from simulations of qNLS and WKE at $t = 2\tau_{kin}$ or $s = 2$ for different values of parameter p . (Right Panel) L_2 -norm of a mismatch between qNLS and WKE as a function of $\Delta k \sim 2\pi/L$ for the case $p = 1.4$ at $s = 2$.

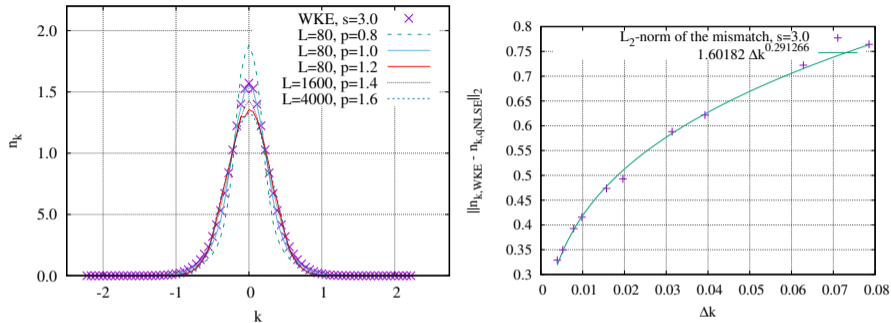


Figure: (Left panel) Comparison of averaged squared amplitudes of harmonics from simulations of qNLSE and WKE at $t = 3\tau_{kin}$ or $s = 3$ for different values of parameter p . (Right Panel) L_2 -norm of a mismatch between qNLSE and WKE as a function of $\Delta k \sim 2\pi/L$ for the case $p = 1.4$ at $s = 3$.

Compare results close to threshold of applicability $p = 1$.

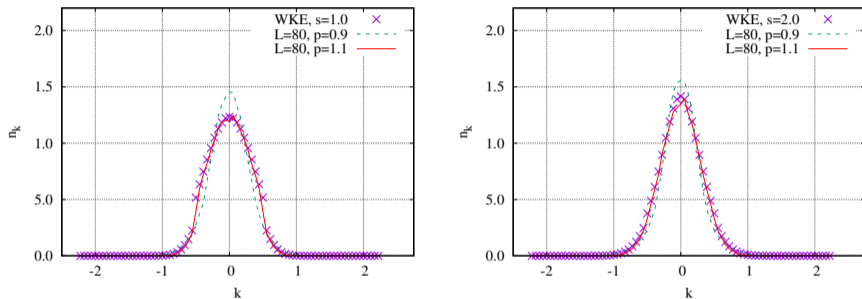


Figure: Solutions of qNLSE at different times for $p = 0.9$, slightly below the threshold in (7) and for $p = 1.1$, slightly above the threshold in (7). In both cases $L = 80$. (Left Panel) Moment of time $t = \tau_{kin}$ or $s = 1$. (Right panel) Moment of time $t = 2\tau_{kin}$ or $s = 2$.

Check of the main assumption of WTT: $\langle a_k a_{k'}^* \rangle = n_k \delta(k - k')$

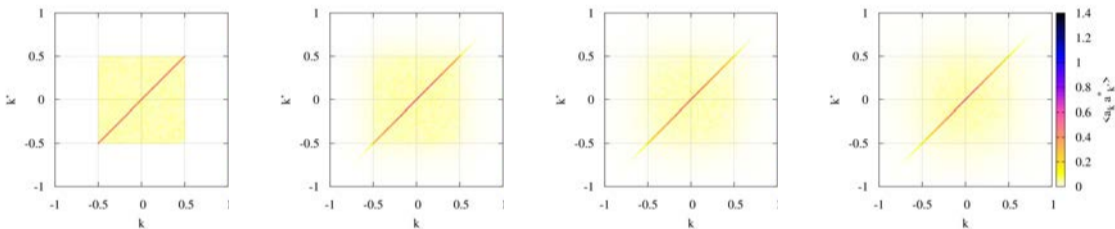


Figure: Pair correlator $\langle a_k a_{k'}^* \rangle$ computed for ensemble of 1000 realizations of initial conditions for qNLSE. Period of the system $L = 200$. The leftmost panel is the initial condition, then $\tau = 1$, $\tau = 2$, and $\tau = 3$. One can observe broadening of the spectrum, but the δ -function approximation is working very well.

Check of the main assumption of WTT: $\langle a_k a_{k'}^* \rangle = n_k \delta(k - k')$

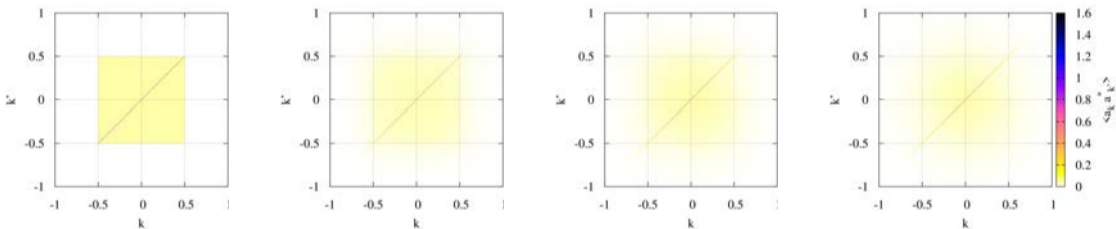


Figure: The same as before, but the period of the system is $L = 800$. One can see the more narrow correlation line, which means that its width is limited only by wavenumbers resolution $\Delta k = 2\pi/L$.

Comparison with Dirichlet BCs. $p = 1.1$, $L = 19$.

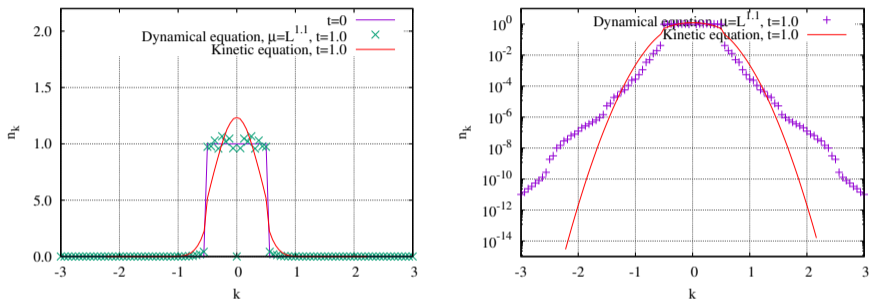


Figure: Comparison of averaged squared amplitudes of harmonics from dynamical simulations with results of simulations in the framework of kinetic equation. Linear and logarithmic scales. Moment of time $s = 1.0$, $p = 1.1$, $L = 19$.

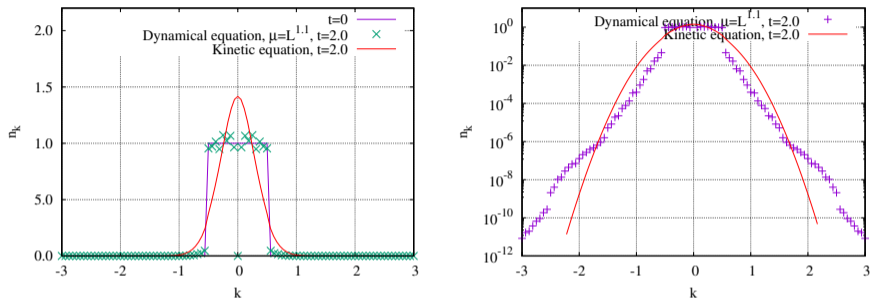


Figure: Comparison of averaged squared amplitudes of harmonics from dynamical simulations with results of simulations in the framework of kinetic equation. Linear and logarithmic scales. Moment of time $s = 2.0$, $p = 1.1$, $L = 19$.

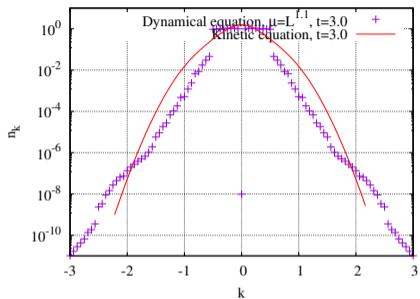
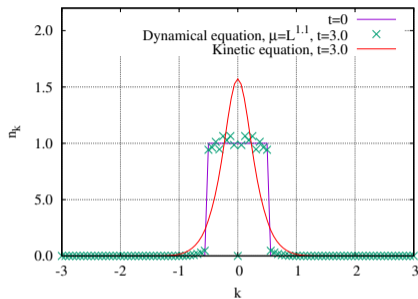


Figure: Comparison of averaged squared amplitudes of harmonics from dynamical simulations with results of simulations in the framework of kinetic equation. Linear and logarithmic scales. Moment of time $s = 3.0$, $p = 1.1$, $L = 19$.

$$\text{Dirichlet BCs: } \langle a_k a_{k'}^* \rangle = n_k \delta(k - k')$$

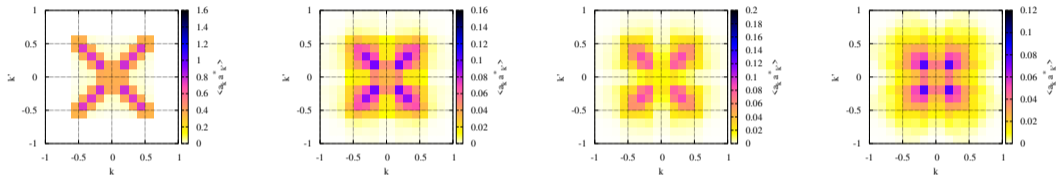


Figure: Pair correlator $\langle a_k a_{k'}^* \rangle$ computed for ensemble of 1000 realizations of initial conditions for qNLSE. Period of the system $L = 19$. The leftmost panel is the initial condition, then $\tau = 1$, $\tau = 2$, and $\tau = 3$. No δ -function approximation!

$$\text{Dirichlet BCs: } \langle a_k a_{k'}^* \rangle = n_k \delta(k - k')$$

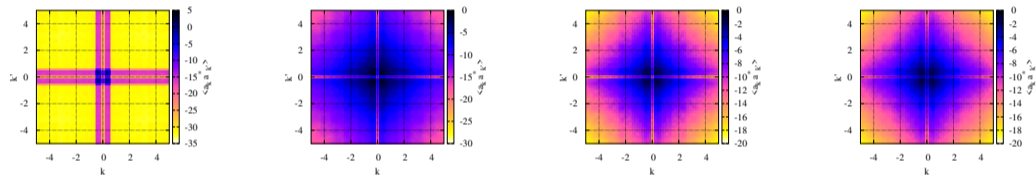


Figure: Pair correlator $\langle a_k a_{k'}^* \rangle$ computed for ensemble of 1000 realizations of initial conditions for qNLSE. Period of the system $L = 19$. The leftmost panel is the initial condition, then $\tau = 1$, $\tau = 2$, and $\tau = 3$. No δ -function approximation!

Results and future work.

- Rigorous derivation of 6-waves WKE for periodic BCs was performed.
- Applicability condition for WKE in periodic case were formulated.
- Break up of WKE with the change of the parameters was demonstrated (too small L results were omitted).
- Break up of WKE for Dirichlet BCs.
- Future work includes:
 - Direct check of other assumptions of WKE derivation.
 - Influence of different BCs.